

1 **Impact of Influent Carbon to Phosphorus Ratio on Performance and** 2 **Phenotypic Dynamics in Enhanced Biological Phosphorus Removal (EBPR)** 3 **System - Insights into Carbon Distribution, Intracellular Polymer** 4 **Stoichiometry and Pathways Shifts**

5 Nehreen Majed^{1,2} and April Z. Gu^{2,3*}

6 ¹ Present Address: Department of Civil Engineering, University of Asia Pacific, 74/A Green Road, Dhaka-1205,
7 Bangladesh. Email: nehreen-ce@uap-bd.edu

8 ²Department of Civil & Environmental Engineering, Northeastern University, 360 Huntington Avenue, Boston, MA
9 02115, USA

10 ^{3*} Corresponding author, Present Address: School of Civil and Environmental Engineering, Cornell University, Ithaca,
11 NY 14853, USA. Email: aprilgu@cornell.edu

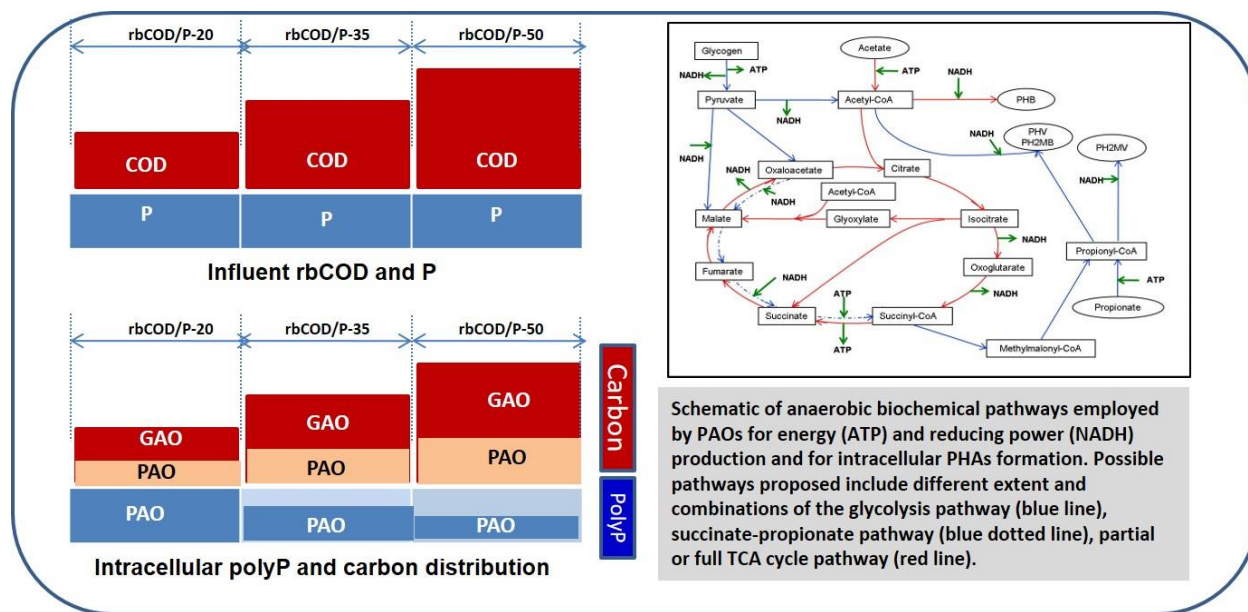
12

13 **Abstract**

14 This study investigated the impact of influent carbon to phosphorus (P) ratio on the variation in
15 P-removal performance and associated intracellular polymers dynamics in key functionally
16 relevant microbial populations, namely, PAOs and GAOs, at both individual and populations
17 levels, in laboratory scale sequencing batch reactor-EBPR systems. Significant variations and
18 dynamics were evidenced for the formation, utilization and stoichiometry of intracellular
19 polymers, namely polyphosphate, glycogen and Polyhydroxyalkanoates in PAOs and GAOs in
20 the EBPR systems that were operated with influent C/P ranged from 20 to 50, presumably as
21 results of phylogenetic diversity changes and, or metabolic functions shifts in these two
22 populations at different influent C/P ratios. Single cell Raman micro-spectroscopy enabled
23 quantification of differentiated polymer inclusion levels in PAOs and GAOs and, showed that as
24 the influent rbCOD/P ratio increases, the excessive carbon beyond stoichiometric requirement
25 for PAOs would be diverted into GAOs. Our results also evidenced that when condition becomes
26 more P limiting at higher rbCOD/P ratios, both energy and reducing power generation required

1 for acetate uptake and PHB formation might shift from relying on both polyP hydrolysis and
 2 glycolysis pathway, to more enhancement and dependence on glycolysis in addition to
 3 partial/reverse TCA cycle. These findings provided new insights into the metabolic elasticity of
 4 PAOs and GAOs and their population-level parameters for mechanistic EBPR modeling. This
 5 study also demonstrated the potential of application of single cell Raman micro-spectroscopy
 6 method as a powerful tool for studying phenotypic dynamics in ecological systems such as
 7 EBPR.

8 **KEYWORDS** Enhanced biological phosphorus removal, EBPR, Raman microscopy,
 9 polyphosphate, PHB, glycogen



11 1. Introduction

12 The increasingly stringent limits imposed on wastewater effluent phosphorus demand for higher-
 13 level treatments through more reliable and better optimization of phosphorus removal processes.
 14 Although enhanced biological phosphorus removal (EBPR) process is considered a potentially
 15 efficient process with economic and environmental advantages compared to traditional chemical

1 phosphorus removal, the benefits are often offset, in practice, by the needs to have standby
2 chemicals for achieving reliable and consistent performance. There is still knowledge gap in
3 understanding the mechanism and factors that control the stability of the process, particularly for
4 achieving extremely low effluent limits and, as a result, process stability and system performance
5 have been seen to vary among facilities (Gu et al., 2005; Neethling et al., 2005; Stephens et al.,
6 2004).

7 EBPR performance and stability have been shown to be affected by many factors among
8 which, the competition of the two main functionally relevant populations, namely polyphosphate
9 accumulating organisms or PAOs and glycogen accumulating organisms or GAOs, were found
10 to be crucial for achieving successful operation of EBPR. Although deterioration of EBPR
11 performance has been attributed to the proliferation of GAOs in lab-scale EBPRs and also at full
12 scale EBPR facilities (Gu et al., 2005; Cech and Hartman, 1993; Saunders et al., 2003), others
13 (Gu et al., 2008; Tu and Schuler, 2013) have also shown that efficient EBPR could also be
14 achieved with relatively high abundance of GAOs being present, highlighting the need for
15 further understanding of the impact of GAOs on EBPR. In addition, the phylogenetic identities,
16 phenotypic elasticities, and biochemical metabolic pathways involved in these two groups of
17 microorganisms are still not fully understood. There are still uncertainties regarding the
18 mechanism and metabolic pathways in the EBPR process; particularly, the involvement of either
19 TCA cycle or glycolysis pathway (Entner-Doudoroff versus Embden-Meyerhof-Parnas pathway)
20 for energy and reducing power generation and, the extent of possession and utilization of these
21 pathways by different phylogenetic PAOs or GAOs groups under various conditions remain
22 unclear (Zhou et al., 2010). Interestingly, recent studies pointed out that these two groups could

1 change and switch their phenotypes and metabolic pathways under different conditions revealing
2 their metabolic flexibility (Acevedo et al., 2012; Lanham et al., 2013; daSilva et al., 2018).

3 Understanding and designing the conditions that are favorable for PAOs over GAOs and
4 other competing microorganisms is considered necessary to maintain the system stability and
5 performance (Neethling et al., 2005; Barnard et al., 2005). Several factors have been shown to
6 impact the competition between PAOs and GAOs, including influent bio-available carbon to P
7 ratio, solid retention time, VFA loading rate, feeding strategy and composition, hydraulic
8 retention time, temperature, pH, dissolved oxygen and, salinity etc. (Cech at Hartman, 1993; Tu
9 and Schuler, 2012; Whang and Park, 2006; Liu et al., 1997; Filipe et al., 2001; Lopez-Vasquez et
10 al., 2009). Among these, the influent C/P ratio is particularly important since it has been
11 correlated with EBRP performance and stability (Gu et al., 2008). The observed stoichiometric
12 requirement of carbon for a unit amount of phosphorus to be removed has been around 10-20 mg
13 rbCOD/mg P removed (Barnard et al., 2005; Tchobanoglous, 2003). Higher rbCOD/P ratios (40-
14 50 mg-rbCOD/mg-P) have been seen to be associated with GAO dominated culture (Liu et al.,
15 1997; Broughton et al., 2008; Kong et al., 2002; Schuler and Jenkins, 2003; Oehmen et al., 2007)
16 and lower ratios (<10-20 mg-rbCOD/mg-P) have been associated with PAO dominated culture.
17 The range of rbCOD/P ratio for satisfying P removal in Water reclamation facilities was
18 recommended as 15:1-25:1 (Randall et al., 1992; Tetreault et al., 1986). Gu et al (2008)
19 hypothesized that although the excessive amount of available carbon can harbor the proliferation
20 of GAOs, stable process can be maintained as long as the operational conditions are controlled to
21 kinetically favor the growth of PAOs over GAOs.

22 The link of influent rbCOD/P ratio with microbial population structures and consequent
23 impact on EBPR performance stability warrants further investigation. Specifically, the impact of

1 varying rbCODd/P loading conditions on the relative abundances of both PAOs and GAOs along
2 with their metabolic changes and competition requires better understanding. The unavailability
3 of diverse PAO and GAO isolates, and the lack of tools to monitor the metabolic state of these
4 two key populations in a mixed culture, make it often difficult to understand the influence of
5 process parameters on the specific population levels. A single cell Raman micro-spectroscopy
6 method that allows for phenotype-based quantification of relative PAO and GAO abundance,
7 simultaneous intracellular detection and quantification of polymers (i.e. polyphosphate, PHB and
8 glycogen) at individual cellular level was developed by Majed et al. (2009, 2010). Later on,
9 Raman-based phenotypic operational phenotype unit (OPUs) was also linked with operational
10 taxonomic unit (OTUs) by Li et al (2018). In this study, we further employed the developed
11 Raman microscopy method to evaluate the impact of influent rbCOD/P ratio on the EBPR
12 system, including overall performance, relative PAO/GAO population abundance and,
13 particularly, on the intracellular polymer dynamics at both single cellular and population levels.
14 These results provided new insights into metabolic diversity, involvement of biochemical
15 pathways and the mechanisms of EBPR.

16 **2. Material and Methods**

17 ***2.1 Sequencing batch EBPR reactors***

18 Three identical lab-scale SBR-EBPR systems were operated with three different influent
19 rbCOD/P ratios of 20, 35 and 50 (ratios relevant to full-scale EBPR processes in US),
20 respectively by changing the influent COD concentrations in relative to constant influent orthoP
21 level of 10 mg-P/L. The SBRs were controlled at a constant room temperature of 19-22°C and
22 operated with four six-hour cycles per day with each cycle consisting of: 10 minutes' fill
23 followed by 130 minutes of anaerobic phase, 183 minutes of aerobic phase, 30 minutes of

1 settling and then 7 minutes of withdrawing. The composition of synthetic wastewater feed was
2 according to Schuler and Jenkins (2003). Phosphorus was added as 45 mg/L sodium phosphate
3 monobasic ($\text{NaH}_2\text{PO}_4 \cdot \text{H}_2\text{O}$) (10 mg-P/L). Influent organic feeding ranging from 200 – 500 mg
4 COD/L as sodium acetate ($\text{CH}_3\text{COONa} \cdot 3\text{H}_2\text{O}$) was provided with supplement of 15 mg/L of
5 casamino acids. We recognize that this study only focused on acetate-fed system that are
6 dominated by *Accumulibacter*-like PAOs and investigation of EBPR systems with more complex
7 carbon feed (i.e mixture of acetate and propionate) is warranted for future studies. Nitrogen was
8 added as ammonium chloride (NH_4Cl) to maintain stoichiometric requirement of nitrogen for
9 growth (rbCOD:N:P of 100:5:1). Allylthiourea was added at 2 mg per liter of feeding to inhibit
10 nitrification. The SRT and HRT of the system were maintained at 7 days and 12 hours
11 respectively. For each rbCOD/P ratio, the SBR was operated for duration of at least 3 times SRT
12 (21-25 days) for obtaining stable performance before subjecting to populations' study and
13 Raman analysis.

14 ***2.2 EBPR performance evaluation***

15 Three SBRs were operated with rbCOD/P ratios of 20, 35 and 50 respectively. For each
16 rbCOD/P ratio operations, P release and uptake cycles were monitored during the steady state
17 period to determine the EBRP activities, including P release and uptake rates, P release to acetate
18 uptake ratios and glycogen degradation to acetate uptake ratios. Samples (in duplicate) were
19 taken at the beginning and at the end of anaerobic cycle and at the end of aerobic cycle for each
20 of the three SBRs with varying influent rbCOD/P ratios for Raman analysis, as well as for
21 quantifying cellular-level intracellular polymers content including polyphosphate, PHB and
22 glycogen. In addition, samples were collected at 15-60 minutes' intervals for bulk chemical
23 analysis to be performed for soluble orthophosphate, total phosphate, acetate, total solids and

1 glycogen content in sludge. The filtered samples through 0.45 μm filter papers were analyzed for
2 orthophosphate (orthoP; $(\text{PO}_4^{3-})^-$) and acetate (CH_3COO^-) using DX-120 ion chromatograph
3 (Dionex Benelux, Belgium). All phosphorus fractions were measured according to the standard
4 method (4500-P) (APHA, 1998). Glycogen was measured according to the method specified by
5 Erdal (2002).

6 **2.3 PAOs/GAOs population analysis**

7 Presence of PAOs in the reactor was confirmed with phosphate removal performance evaluation,
8 Neisser and DAPI staining (Jenkins et al., 1993; Streichan et al, 1990) for total PAO observation
9 and, FISH for detecting known candidate PAOs and GAOs. Oligonucleotide probes targeting
10 *Accumulibacter* PAOs, *Actinobacteria* PAOs, *Competibacter* GAOs, *Defluvicoccus* clusters 2
11 GAOs were used in FISH analysis (Detailed listing of probes is provided in STable 1). The
12 staining, FISH protocol and hybridization conditions used were previously described (He et al.,
13 2008; Zilles et al., 2002). DAPI staining for polyP was carried out at 50 $\mu\text{g}/\text{ml}$ of DAPI for 1
14 min, whereas, DAPI staining for total population in hybridized slides (to analyze for relative
15 abundance of phylogenetic sub-groups of PAOs and GAOs over total population) was carried out
16 at 1 $\mu\text{g}/\text{ml}$ of DAPI for 10 min. Hybridized and DAPI stained cells were observed with an
17 epifluorescent microscope (Zeiss Axioplan 2, Zeiss, Oberkochen, Germany). For the
18 quantification of the relative proportion of the target types of cells, around 20 micrographs were
19 collected with random fields of view from the same slide/sample and average abundance of the
20 target cells was calculated as the relative proportion of fluorescing area having the target label
21 (PAO/GAO) compared to the area of the total population (DAPI) using DAIME (Digital Image
22 Analysis in Microbial Ecology) software version 1.3.1 (<http://www.microbial-ecology.net/>)
23 (Daims et al., 2006). The standard error of the mean (SEM) was calculated as the standard

1 deviation of the area percentages divided by the square root of the number of images analyzed.
2 For Raman analysis, fractions of target populations (PAOs/GAOs) were determined by averaging
3 the fractions of samples from aerobic phase according to Majed et al (2012).

4 ***2.4 Raman Micro-Spectroscopy Analysis***

5 Samples subjected to Raman analysis were prepared on optically polished CaF₂ windows (Laser
6 Optex, Beijing, China) according to Majed et al (2010). Samples were homogenized rigorously
7 by 26-gauge needle and syringe to obtain a more uniform sample. Raman spectra for at least 40-
8 45 single cells were examined for each sample and the sample size was determined with
9 consideration of both the desired accuracy and labor-intensiveness of the Raman analysis.
10 Statistical analysis of the sample size and validation of the analysis accuracy and reliability was
11 demonstrated in our previous publications (Majed et al., 2010; Li et al., 2018) and also provided
12 in supporting information (SFigure 3 and SFigure 4). Raman spectra were acquired using a
13 WITec, Inc. (Ulm, Germany) Model CRM 2000 confocal Raman microscope. Excitation (ca. 30
14 mW at 633nm) was provided by a Helium/Neon laser (Melles Griot, Carlsbad, CA). Details on
15 the acquisition of spectra can be obtained in Majed et al. (2009). Relative quantity of polyP
16 content in each individual cell was evaluated based on the Raman intensity (peak height in the
17 unit of Charged Coupled Device (CCD counts) of the PO₂⁻ stretching band occurring around
18 1168-1175 cm⁻¹ wave number region after background correction (Majed et al., 2009). The C=O
19 stretching band of ester linkage occurring around 1734 cm⁻¹ and glycogen vibration occurring
20 around 480 cm⁻¹ were used for quantification of PHB and glycogen content, respectively (Majed
21 and Gu, 2010). Total PHV concentration associated with the two populations could not be
22 quantified via Raman due to the overlapping of peak positions between PHV and glycogen
23 (Majed and Gu, 2010). Depending on the time point during the anaerobic/aerobic EBPR cycle

1 when the sample was taken, and the expected corresponding Raman polymers spectrum based on
 2 current understanding of the EBPR mechanisms and polymer functions, cells containing polyP,
 3 with or without other polymers (glycogen, PHA) were categorized as PAOs and the cells
 4 containing only glycogen or combination of glycogen and PHA, were assigned as GAOs.
 5 Detailed description of the rationale and validation of the proposed quantification methods is
 6 referred to Majed et al. (2012).

7 **3. Results and Discussion**

8 ***3.1 Impact of Influent rbCOD/P on EBPR performance and kinetics***

9 Table 1 shows the EBPR activities-related stoichiometry observed in EBPR systems along with
 10 the performance and stability of the system at different influent feeding rbCOD/P ratios.
 11 Operational data for the SBRs under monitoring (STable 2) indicated that percent removal of P
 12 changed from 82% to 95% to 97% as rbCOD/P ratio changes from 50 to 35, then to 20
 13 respectively. The results showed good P removal at rbCOD/P ratio of 20 to 35, and significant
 14 decrease in P removal efficiency at rbCOD to P ratio of 50.

15 **Table 1: P removal performance and activity data of the SBR- EBPR systems operated with influent**
 16 **rbCOD/P ratio at 20, 35 and 50, respectively**

Influent mg- COD/m g-P	Cumulative Frequency Effluent ortho-P< 1mg P/L	Cumulative Frequency of Effluent ortho-P< 0.5mg P/L	P Removal Efficiency (%)	P release rate, mg- P/gVSS.h	P uptake rate, mg- P/gVSS. h	P _{release} /HAc uptake Pmol/Cmol	Gly _{utilization} / HAc _{uptake} Cmol/Cmol	P content, mg-P/mg- VSS
20	0.85	0.6	97	50.63	23.81	0.6	0.41	0.09
35	0.86	0.63	95	38.14	21.2	0.47	0.74	0.06
50	0.5	0.31	82	4.38	9.82	0.22	1.04	0.024

1
2 Through comparison of cumulative frequency of the occurrence that effluent orthoP is obtained
3 below <1 mg/L and below <0.5 mg/L, the system with COD/P ratio of 35 ensures the maximum
4 stability while the system with rbCOD/P ratio of 20 performs almost similar. However, system is
5 far from stable for the SBR system with rbCOD/P ratio of 50.

6 According to established EBPR models, EBPR metabolic pathways demand certain
7 stoichiometric relationships among the storage polymers. The $P_{\text{release}}/HAc_{\text{uptake}}$ (P/HAc) ratio is
8 often used as an indicator of the relative PAO and GAO activities and abundance. As shown in
9 Table 3, the P/HAc ratio was 0.6 Pmol/Cmol for rbCOD/P ratio of 20 which decreases linearly
10 with increasing rbCOD/P ratio. Previous studies indicated that higher influent rbCOD/P led to
11 more GAO-dominant microbial population in the system (Smolders et al., 1994). This is
12 confirmed and supported by our population analysis results that are discussed in the section 3.2.

13 The anaerobic glycogen_{utilization}/HAc_{uptake} ratios (Gly/HAc ratio) decreased linearly from 0.41 to
14 1.04 Cmol/Cmol from rbCOD/P ratio of 20 to 50 respectively. These ratios are within the range
15 between TCA cycle and glycolysis activity, as reported in full-scale EBPR facilities and also in
16 established models for PAOs and GAOs (Gu et al., 2008; Lanham et al., 2013; Smolders et al.,
17 1994; Zeng et al., 2003). The increase of Gly/HAc indicates a preferential reliance by the
18 population on TCA cycle at a lower rbCOD/P to an increased reliance on the glycolysis pathway
19 at a higher rbCOD/P. Similar scenario has been observed in several EBPR facilities in Denmark
20 (Lanham et al., 2013). In addition, decrease in the overall P content from 0.09 to 0.024 mg-P/mg-
21 VSS (with increasing rbCOD/P) indicate a decrease in the relative population of PAOs with
22 increasing rbCOD/P ratio.

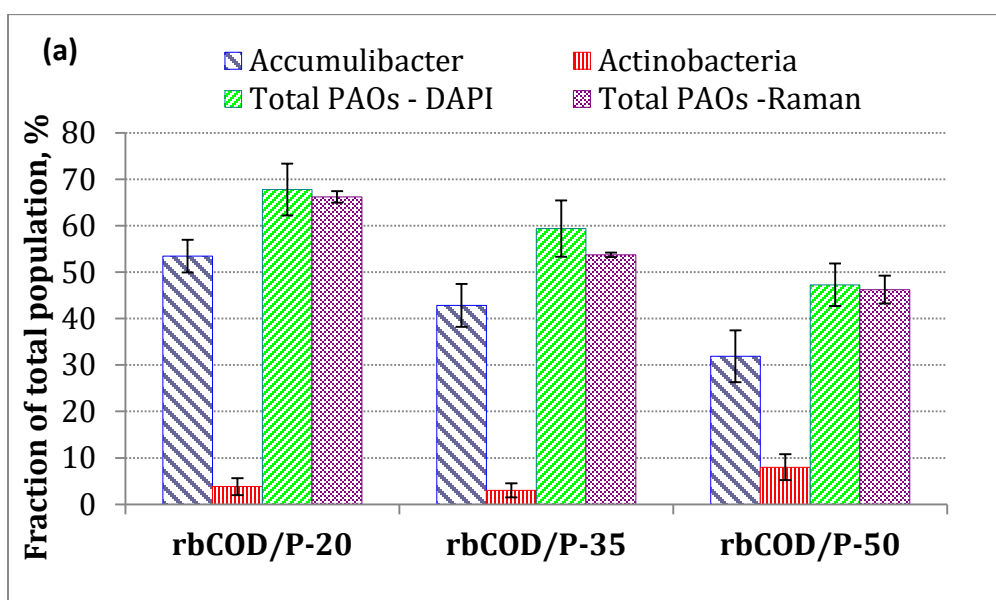
23

1 **3.2 Impact of influent rbCOD/P on relative PAO- GAO population abundance and Association**
2 **with EBPR activities**

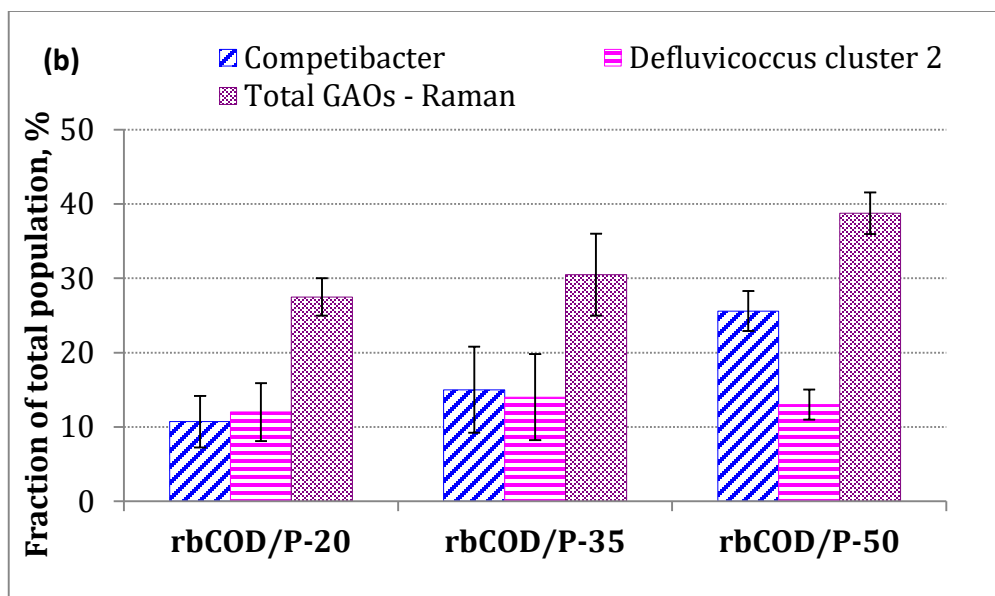
3 Figure 1 shows the PAOs (Figure 1a) and GAOs (Figure 1b) population fractions changes in
4 response to varying influent rbCOD/P ratios, using conventional DAPI staining, FISH
5 measurements and Raman analysis. As shown in Figure 1a, total PAOs determined via Raman
6 spectrum agreed well with those estimated by DAPI staining for all rbCOD/P ratios. Currently,
7 there is no other method available for quantifying total GAOs in EBPR systems; therefore, the
8 GAOs abundance determined by Raman could not be compared. Note that the sum of GAOs and
9 PAOs, as quantified by Raman analysis, comprised around 85-90% of total microbial population
10 in the SBR-EBPR studied, indicating that our methods captured majority of the population.

11 Both *Accumulibacter*-like PAOs and total PAOs abundance decreased, as the influent
12 rbCOD/P (mg-COD/mg-P) ratio increased from 20 to 50 (Figure 1a). *Accumulibacter* PAOs
13 comprised around 70% of total PAOs population at all rbCOD/P ratios studied. *Actinobacteria*
14 type PAOs constituted a minor fraction of total PAOs being less than 5% of the total population
15 at rbCOD/P ratios of 20 and 35, however, their abundance increased to 8% at rbCOD/P of 50.
16 *Actinobacteria* PAOs are known to grow on amino acids instead of acetate and the casamino
17 acids in the feeding likely provided the amino acid source that supported the growth of
18 *Actinobacteria*. Concurrently with the decrease of relative PAOs abundance, the relative GAOs
19 abundance increased by 40% with the increasing rbCOD/P ratios from 20 to 50 as shown in
20 figure 1b. *Alphaproteobacterial Defluvicoccus* cluster 2 (DF2) and *Competibacter* type GAOs
21 accounted for majority (>80%) of the total GAOs (based on Raman measurements since there is
22 currently no other method available for quantifying total GAOs) in our culture (Figure 1b).
23 *Competibacter* abundance increased by >40% with the increasing rbCOD/P ratios from 20 to 50,

1 but abundance of DF2 did not seem to vary, indicating that *Competibacter* was likely the one
2 that responded to the change in loading ratio. Muszyński and Miłobędzka (2015) also observed
3 increase in *Competibacter* abundance from 4 to 20% when the rbCOD/P ratio was changed from
4 15:1 to 100:1 with aerobic granular sludge while abundance of *Alphaproteobacterial*
5 *Defluvicoccus* cluster 1 (DF1) remained constant at 2% (they did not detect DF2 type GAOs in
6 the granular sludge). These results clearly showed that both relative abundance and community
7 compositions of PAOs and GAOs shifted as the influent rbCOD/P ratio changed.



8



1
2 **Figure 1: Abundances of population fractions belonging to the groups (a) PAOs and (b)**
3 **GAOs at different rbCOD/P ratios quantified via DAPI staining (total PAOs), FISH**
4 **(known candidate sub-PAOs and GAOs) and Raman polymers spectrum analysis (total**
5 **PAOs and GAOs based on intracellular polymers). Error bars represent standard error**

6 The changes in relative abundance of PAOs and GAOs in response to influent rbCOD/P
7 variations were consistent with the chemical analysis of P content level in the sludge and the
8 evaluation of EBPR activities, as summarized in Table 1 (profiles demonstrated in SFigure 1).
9 With a higher carbon loading with respect to phosphorus, the P content in sludge, the P release
10 rate and the $P_{\text{release}}/HA_{\text{uptake}}$ ratios decreased, indicating a decline of relative PAOs activities
11 (presumably proportional to PAO populations) and increase in relative GAOs in the sludge.
12 Correlation analysis of relative PAOs abundance (%) with the EBPR activities parameters
13 seemed to indicate that relative total PAOs abundance change correlated more
14 significantly ($p < 0.05$) with $P_{\text{release}}/HA_{\text{uptake}}$ ratio ($r = 0.99$, $p = 0.0351$) and sludge P content ($r =$
15 0.99 , $p = 0.0468$), but less so with P release rate ($r = 0.99$, $p = 0.0991$),
glycogen_{degradation}/ HA_{uptake} ratio ($r = -0.99$, $p = 0.0836$), and P uptake rate ($r = 0.97$, $p = 0.155$).

1 The result also showed positive correlation between the P_{rel}/HAc_{uptake} ratio and the abundance
2 ratio of *Accumulibacter*/*(Competibacter+DF2)* (correlation coefficient, $r = 0.97$; $p = 0.1553$), as
3 well as P_{rel}/HAc_{uptake} ratio and total PAO/GAO (analyzed by Raman) ($r = 0.98$, $p = 0.1248$) at
4 different rbCOD/P ratios.

5 Previous studies have indicated that rbCOD/P ratio seem to dictate the relative PAO and
6 GAO population abundance based on indirect observation of changes in EBPR activities (since
7 total GAOs could not be quantified previously) (Gu et al., 2008; Liu et al., 1997; Schuler et al.,
8 2003). Our results are consistent with the previous studies, and more clearly demonstrated the
9 impact of rbCOD/ P ratio on both total and different sub-populations of PAO and GAOs, as well
10 as their associated phenotypic activities. We recognize that this study only focused on acetate-fed
11 system that are dominated by *Accumulibacter*-like PAOs and investigation of EBPR systems with
12 more complex carbon feed (i.e mixture of acetate and propionate) is warranted for future studies.

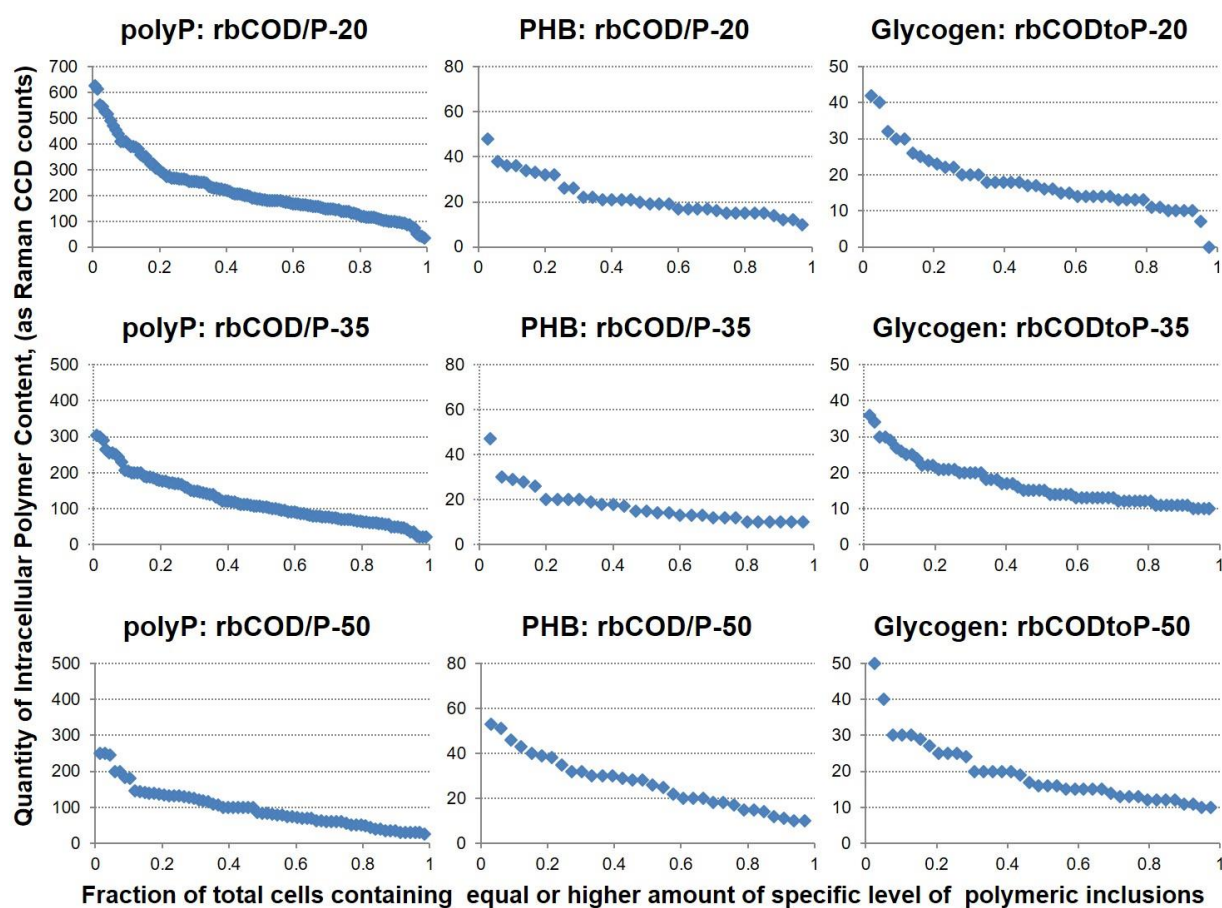
13 One intriguing observation is that P removal performance deteriorated at rbCOD/P ratio
14 of 50, even though the system still contained rather high relative abundance of total PAO and
15 *Accumulibacter*-like PAOs (47%, 32% respectively.), which are higher than typical range
16 observed at full-scale EBPR systems (Neethling et al., 2005; Gu et al., 2008; Lanham et al.,
17 2013; Gu et al., 2018). This suggests, in agreement with previous observations, that EBPR
18 performance does not always correlate with relative PAOs abundance alone.

19 ***3.3 Impact of Influent rbCOD/P ratio on population- level distributions of intracellular*** 20 ***polymer content in PAOs and GAOs***

21 Raman analysis allows for the quantification of intracellular inclusion of polyP, PHB and
22 glycogen within each individual cell and therefore can reveal the level and distribution of
23 intracellular polymer contents among populations. In addition, by identifying the cells as either

1 PAOs or GAOs based on their unique polymer combination as described previously, the changes
2 and dynamics of the functionally relevant intracellular polymers associated with either PAOs or
3 GAOs can be, for the first time, evaluated separately. However, it should be noted that
4 evaluation of the levels of intracellular polymeric inclusions and the resulting distributions do
5 not necessarily correspond to the rate of increase or decrease of polymer formation or
6 degradation at any given condition, nevertheless the variations in the levels at different
7 conditions depict the dynamics of intracellular transformations in response to the influent loading
8 changes.

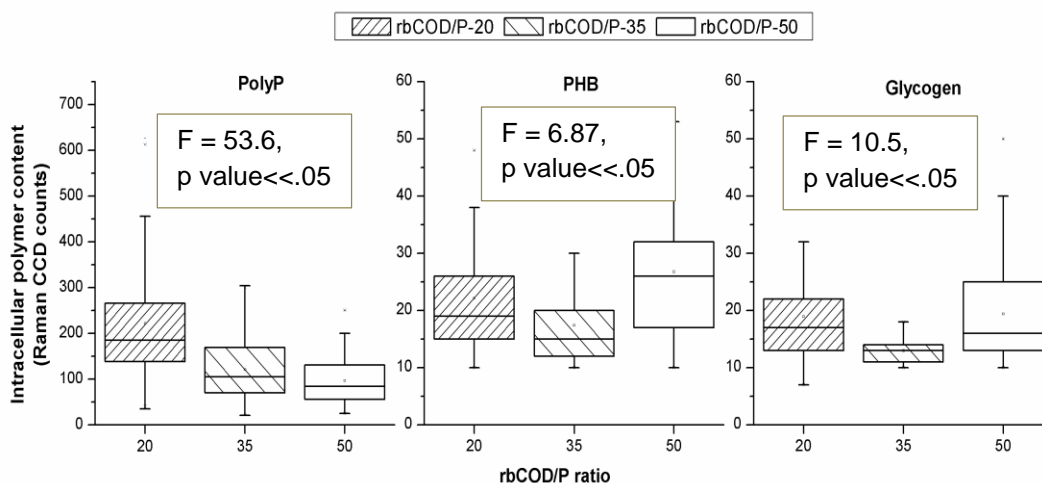
9



10

11

Figure 2: Intracellular polymer content level (intensity as CCD counts) distribution among PAOs cells for polyphosphate, PHB, and glycogen quantities, respectively. Data based on batch testing sampling of all cells subjected to single cell Raman micro-spectroscopy analysis in the three EBPR SBR systems fed with different influent COD/P (mg/mg) ratios. X axis: fractions of cells that contained equal or higher amount of the specific level of polymeric inclusion at any given testing. Y-axis: level of polymeric inclusion in CCD counts.



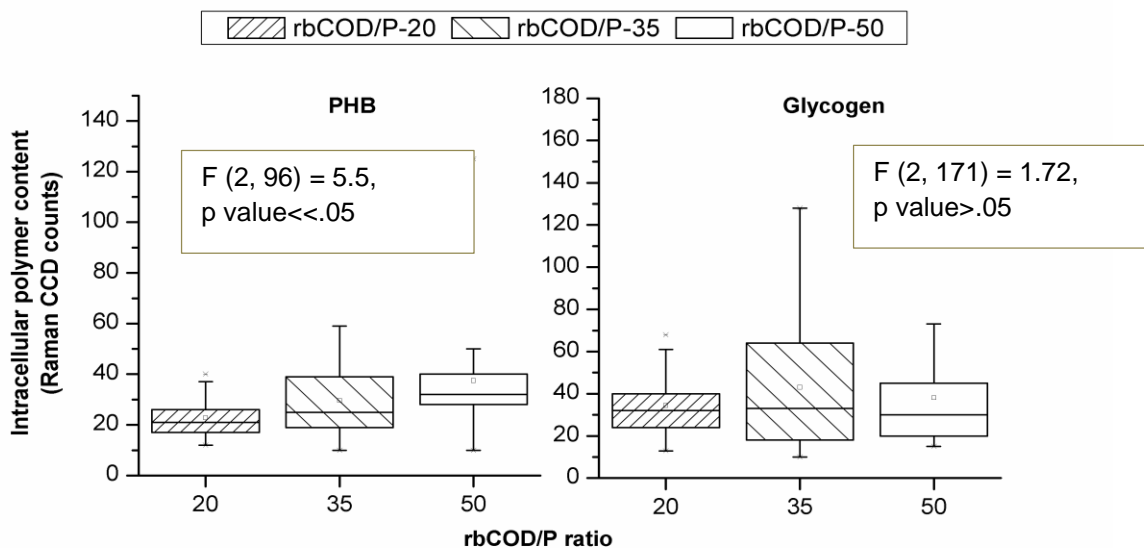
1
2 **Figure 3: Box plots showing the minimum, maximum and median levels of intracellular**
3 **polymer content levels of polyP, PHB and glycogen polymers in individual PAO cells**
4 **revealed by single cell Raman micro-spectroscopy (respective F statistic and P values are**
5 **shown in figures)**

6 Figure 2 and Figure 3 show the comparison of quantity level and distributions of different
7 intracellular polymers in PAOs for EBPR systems operated under three different influent
8 rbCOD/P ratios. Both 50 percentile and maximum polyP intensity inside individual PAO cells
9 decreased as the rbCOD/P ratio increased even though the influent P concentration remained the
10 same (SFigure 1). Drastic decrease of cellular level polyP content at increased rbCOD/P ratio is
11 quite contrary to the traditional assumption in EBPR models that considers that the maximum
12 saturated intracellular polyP levels is relatively constant and only PAO populations abundance
13 varies with the external condition (Streichan et al., 1990). Therefore, PAOs abundance changes
14 based on the bulk sludge P content or overall P release during EBPR process may not be
15 adequate. In contrast to significant polyP abundance changes, the intracellular PHB levels in the
16 PAOs exhibited slight increase (38% for median, 37% for maximum values disregarding the
17 outlier) as the influent rbCOD/P ratio increases from 20 to 50 (Figures 2 and 3). There was no

1 significant change in the median level of intracellular glycogen level in PAOs, however
2 maximum and minimum levels increased (25% and 43% respectively, Figure 3) as rbCOD/P
3 increased from 20 to 50. This warranted the one-way ANOVA test among the polymeric
4 inclusion data which revealed $F_{\text{polyP}}(2,301) = 53.6$, $p < 0.05$; $F_{\text{PHB}}(2,92) = 6.87$, $p < 0.05$;
5 $F_{\text{glycogen}}(2, 119) = 10.5$, $p < 0.05$ for PAOs suggesting that the changes in polymeric inclusion
6 levels with changes in rbCOD/P ratio are statistically significant. This implies that the
7 intracellular polymers content and their stoichiometric ratios in PAOs are rather dynamic
8 depending on the influent carbon loadings, which can be associated with both PAO phylogenetic
9 diversity and phenotypic elasticity. Therefore, the saturation level (maximum) of these
10 intracellular polymers that are considered to be a constant in current EBPR models (Schuler,
11 2005) needs further justification.

12 Similarly, observations of inclusion level and distribution for intracellular glycogen and
13 PHB content in individual glycogen containing cells (GAOs) were revealed by single cell Raman
14 microspectroscopy (Figure 4 and SFigure 2). Significant increase in cellular PHB content (50%
15 increase in median and 31% increase in maximum cellular level) with elevation of rbCOD/P
16 ratios (from 20 to 50) in GAO cells (Figure 4) was observed. Intracellular glycogen level in
17 GAOs exhibited overall increase for maximum levels (50% increase from rbCOD/P of 20 to 50),
18 however median values remained almost similar. This warranted the one-way ANOVA test
19 among the polymeric inclusion data which revealed $F_{\text{PHB}}(2,96) = 5.5$, $p < 0.05$; $F_{\text{glycogen}}(2,171)$
20 $= 1.72$, $p > 0.05$ for GAOs. This suggests the higher carbon loading to the EBRP systems not only
21 resulted in increase of relative abundance of GAOs, but also led to either selection of GAOs with
22 higher intracellular PHB, and/or encouraged GAOs to accumulate more PHA pool inside cells.

- 1 However, the increment of glycogen pool within GAO cells with increase in rbCOD/P ratio is
- 2 not statistically significant.
- 3



4

5 **Figure 4: Box plots showing the minimum, maximum and median levels of intracellular**
6 **polymer content levels of PHB and glycogen polymers in individual GAO cells revealed by**
7 **single cell Raman micro-spectroscopy (respective F statistic and P values are also mentioned)**

8

9 These results, for the first time, revealed the individual cellular level polymers level

10 changes in both PAOs and GAOs populations in response to changes in influent carbon and P

11 loading conditions. These observed intracellular polymers dynamics could result from and reflect

12 the changes in phylogenetic diversity and, or metabolic functions shifts in PAOs, which requires

13 further investigation. The results also imply that there is great heterogeneity of the intracellular

14 polymers storage amount among PAOs and GAOs, which can be dynamic depending on

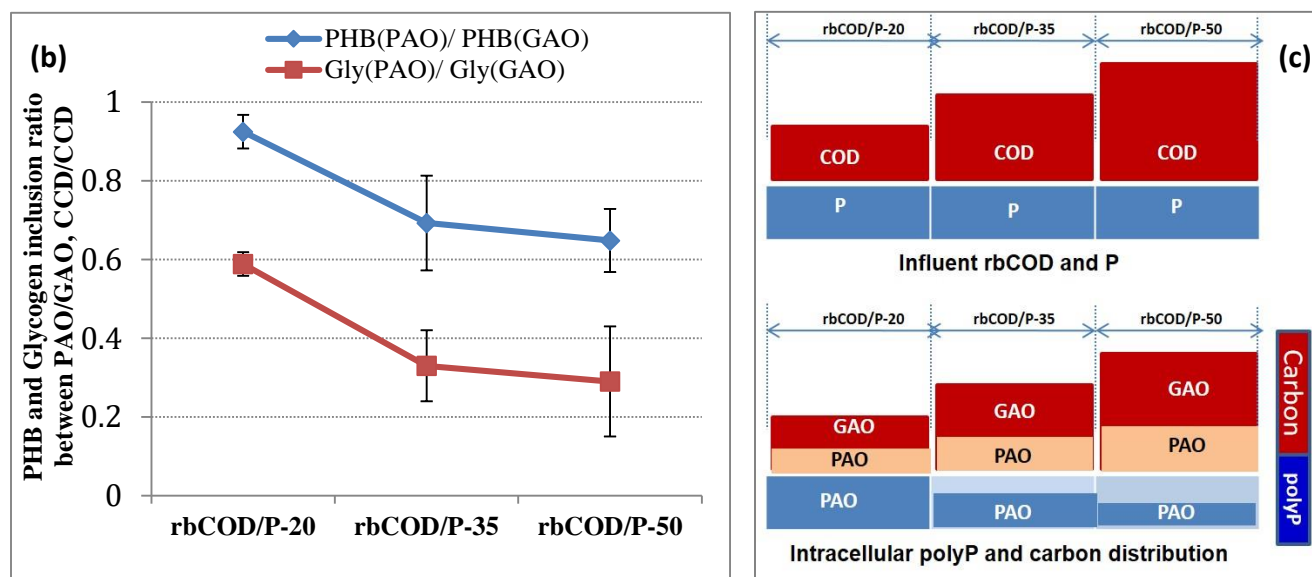
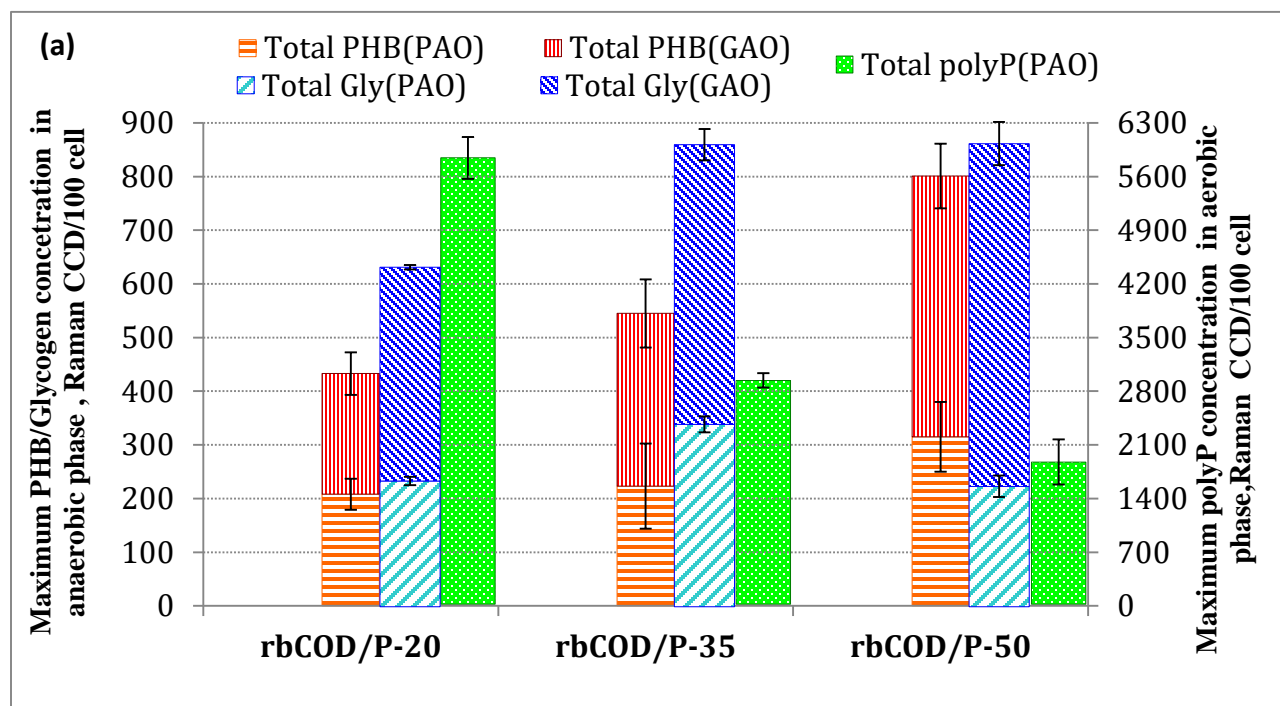
15 operational conditions.

1 ***3.4 Distribution of Carbon and polyP between PAOs and GAOs at varying COD/P condition***

2 Using the Raman-based PAO and GAO identification methods described earlier,
3 differentiated intracellular polymer content associated within PAOs versus those within GAOs
4 could be quantified and evaluated separately (Majed and Gu, 2010). Figure 5a shows the total
5 and distributed PHB (normalized amount at the end of the anaerobic phase when the PHB
6 content is presumably to be at the maximum level) and glycogen content levels (normalized
7 amount at the end of the aerobic phase when the glycogen content is presumably to be at the
8 maximum level) inside PAOs and GAOs. Figure 5b shows the ratio of PHB and glycogen
9 content in PAOs in relative to those in GAOs at different rbCOD/P loading conditions and figure
10 5c is a qualitative illustration of the distribution and carbon flow among PAOs and GAOs in
11 response to the increase in influent carbon loads.

12 Both total PHB and total glycogen concentration in the overall mixed population (sum of
13 those in both PAOs and GAOs) exhibited elevating trends with the increasing rbCOD/P ratio.
14 Majority portion of incremental PHB and glycogen content was associated with GAOs,
15 indicating the flow of the increased carbon to GAOs as a result of increased relative abundance
16 of GAOs as well as elevated average individual cellular glycogen content in GAO cells. The
17 ratio of PHB inside PAOs to that inside GAOs dropped from 0.92 to 0.65 when rbCOD/P ratio
18 increased from 20 to 50, (Figure 5b). These results clearly demonstrated the quantitative shift in
19 intracellular carbon storage distribution between the two populations, from having a good
20 portion (50%) of the total PHB in PAO populations to having majority of the carbon shuttled to
21 GAOs as the rbCOD/P increased. These results support the hypothesis and carbon distribution
22 model proposed by Gu et al (2008) that as the influent rbCOD/P ratio increases, the excessive
23 carbon beyond stoichiometric requirement for PAOs would be diverted into GAOs.

1
2
3
4
5
6
7
8
9



11

Figure 5: (a) Total and distributed intracellular PHB, glycogen and polyP content between PAOs and GAOs in EBPR systems operated with different influent rbCOD/P ratios. The concentration of the polymer inclusions in a given biomass sample was determined as the sum of total polymers amounts in those cells who contain the polymer(s) normalized by the number of total cells analyzed (sample size). PHB, glycogen and polyP content in a biomass sample was measured with samples taken from anaerobic, aerobic and aerobic phases respectively; (b) Ratio of the PHB and glycogen within PAOs to those in GAOs at different COD/P ratios. (Error bars represent the standard deviation between two separate measurements); (c) Qualitative illustration of intracellular carbon storage distribution between PAOs and GAOs in response to varying carbon loading conditions.

1 Also shown in Figure 5a is the normalized polyP concentration (total polyP amount
2 determined by Raman normalized to sample size) that exhibited dramatic decrease with increase
3 in rbCOD to P ratio as a result of decrease in individual cellular polyP intensity. These results are
4 consistent with bulk P content (Table 1), suggesting again the validity of the Raman analysis for
5 polyP. The quantitative measurement of intracellular polymers associated with PAO and GAO
6 populations allowed for the estimation of changes in the stoichiometry of the utilization and
7 formation of these polymers with different loading conditions. Table 2 summarizes the ratios of
8 PHB formation to polyP utilization, glycogen utilization to polyP utilization and PHB formation
9 to glycogen utilization during the anaerobic phases in PAOs. As described in our previous
10 studies, the lack of standard chemicals for polymers and difficulty with Raman method to
11 establish a reference calibration for a mixed culture (activated sludge) as ours did not yet allow
12 the conversion of CCD count to conventional units of mg/L (Majed et al., 2009). Therefore, we
13 could not compare our stoichiometric values directly with those reported in the literature yet
14 (Oehmen et al., 2010). Nevertheless; the ratios used here are still valid for assessing the impact
15 of rbCOD/P ratio on these values. Based on the current biochemical model of EBPR, the
16 theoretical stoichiometric ratios between polyP, PHB and glycogen polymers are generally
17 assumed to be constant for a given pathway within a given population (Smolders et al., 1994).
18 However, as shown in Table 2, each of the ratios varied consistently for PAOs as the loading
19 conditions changed. These results, for the first time, demonstrated that the EBPR stoichiometry
20 could vary significantly with loading conditions, possibly due to the metabolic states changes
21 (e.g utilization of different pathways) and /or population changes within phylogenetic sub-groups
22 (e.g sub clusters of *Accumulibacter*-like PAOs).

23

1 **Table 2: Stoichiometric ratios of polyP utilization, PHB formation and glycogen utilization**
2 **in the anaerobic phase for PAOs, in SBR-EBPR system operated with different influent**
3 **rbCOD/P (mg/mg) ratios.**

	PHB formation / polyP utilization	Glycogen utilization /polyP utilization	PHB formation /Glycogen utilization
	CCD/CCD	CCD/CCD	CCD/CCD
rbCOD/P-20	0.044	0.009	4.84
rbCOD/P-35	0.13	0.07	1.81
rbCOD/P-50	0.24	0.21	1.21

4

5 *3.5 Insights into the metabolic pathways involved in EBPR*

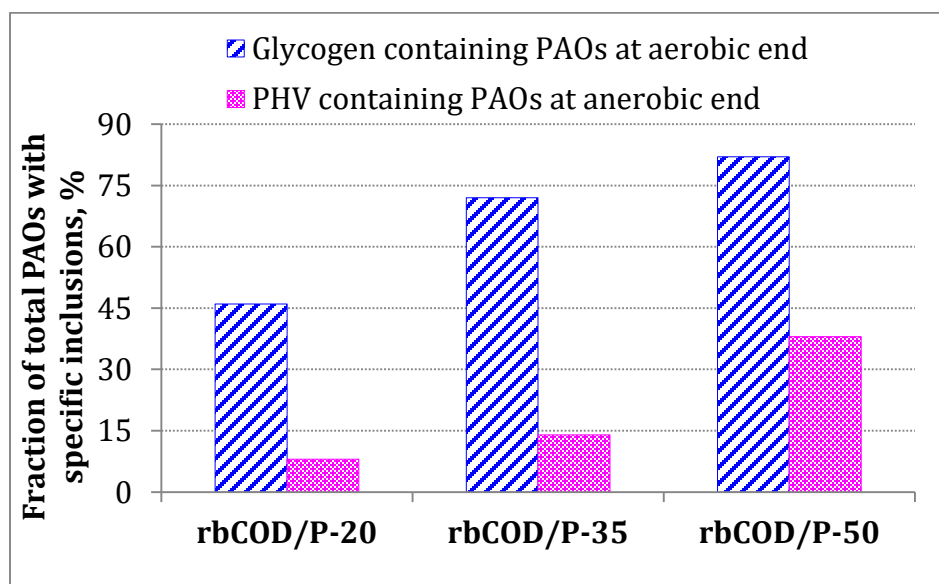
6 Uncertainties still exist regarding the pathways employed by PAOs for reducing power generation
7 in anaerobic EBPR process, which would affect the stoichiometric ratios and the amount and type
8 of PHA formation from acetate uptake (Zhou et al., 2010). Current understanding indicates that
9 PAOs can use glycolysis in addition to partial TCA cycle (reductive branch of TCA cycle, also
10 called succinate-propionyl-coA pathway), split (reverse) TCA cycle and/or glyoxylate shunt based
11 on carbon preservation under different polymer content (daSilva et al., 2018; Martin et al., 2006;
12 Wilmes et al, 2008; He et al., 2010; Zhou et al., 2009) (provided as SFigure 5 and SFigure 6). The
13 extent of involvement and utilization of these pathways also vary depending on the phylogenetic
14 subgroups of PAOs and different external loading/nutrient availability conditions (Zhou et al.,
15 2010; daSilva et al., 2018; Oehmen et al., 2010).

16 Our results suggest that when condition becomes more P limiting at higher rbCOD/P ratios, both
17 energy and reducing power generation required for acetate uptake and PHB formation might
18 shift from relying on both polyP hydrolysis and glycolysis pathway, to more enhancement and
19 dependence on glycolysis in addition to partial/reverse TCA cycle. This is supported by The
20 anaerobic glycogen utilization to polyP utilization ratio inside PAOs which increased nearly 20

1 times from 0.009 to 0.21 as influent rbCOD/P elevated from 20 to 50 (Table 2). This is also
2 consistent with the increasing trend of glycogen_{degradation}/HAc_{uptake} ratio with higher rbCOD/P
3 ratio (Table 1). Furthermore, Figure 6 is a representation of the increase in the fraction of
4 glycogen containing PAO cells (those containing both polyP and glycogen or
5 polyP+glycogen+PHB) in the EBPR system under study and the corresponding increase in the
6 PAO cells that contained PHV as the rbCOD/P ratio increases. Previously established EBPR
7 models (SFigure 5) and current understanding (SFigure 6) assume that PHB can be formed via
8 some form of TCA cycle or glycolysis or combination of both, however, PHV can mainly be
9 formed through glycolysis pathway in combination with the succinate-propionate pathway
10 (reductive branch) of TCA cycle or reverse TCA with glyoxylate shut combined with succinyl-
11 CoA (daSilva et al., 2018) Thus, increase in the PHV containing PAO cells indicates the larger
12 extent of employment of partial/split TCA pathways with increasing rbCOD/P ratio. Previous
13 studies have often associated the increase in PHV content in the EBPR system with increase in
14 the relative population abundance of GAOs since the latter mainly utilize glycolysis pathway and
15 produce higher amount of PHV. However, our results revealed that the fraction of PAOs that
16 contain PHV could vary as well with different operational loading conditions, irrelevant to the
17 abundance of GAOs. Acevado et al (2012, 2017) showed that long-time P limited conditions
18 enhance glycolytic pathway to supply energy deficit and shift towards more GAO-like
19 metabolism. It was observed later by da Silva et al (2018) that when polyP is limited, reverse
20 (split) TCA cycle is the most optimal pathway suggesting GAOs are operating reverse TCA
21 cycle.

22 It should be noted that for individual PAO cells in our study, the relative percentage of
23 PHV content to total PHB+PHV never exceeded 8-12% (data not shown), which is consistent

1 with the PHV content range reported previously with PAO-enriched (>70%) system (Oehmen et
2 al., 2007). These results, for the first time, provided direct cellular and population level evidence
3 for the possibility that at higher rbCOD/P loading condition when P becomes more limited, there
4 were shifts in the involvement of different metabolic pathways in PAOs. Now, whether this was
5 caused by phenotype changes or shifts in phylogenetic sub-populations that possess different
6 pathways still requires confirmation via further investigation. Furthermore, it is also possible that
7 some of these PAO cells might follow certain metabolism that does not involve the known and
8 identifiable storage polymers.



9
10 **Figure 6: Distribution of fractions of PAOs (over total PAOs at respective phases)**
11 **containing PHV at the end of anaerobic phase and glycogen at the end of aerobic phase in**
12 **EBPR systems with different influent rbCOD/P ratios**

12 Conclusion

13 The lack of PAO isolates and the tools to monitor the quantities related to metabolic states of PAOs
14 made it difficult to investigate the speculations that require observation from both phenotypic and
15 phylogenetic aspects. The Raman microscopy method employed in this study helped us gaining

1 further population and cellular level insights into the metabolic diversity among sub-populations
2 within PAO group via tracking of intracellular polymeric inclusions in different metabolic stages
3 of EBPR system, in contrast to the bulk measurements describing the EBPR process that are
4 actually “apparent” sums of different PAOs groups with diverse metabolic pathways. To
5 summarize, the following major conclusions could be drawn:

- 6 • Influent rbCOD/P ratio affected EBPR system stability and relative dominance/abundance of
7 functionally relevant PAOs/GAOs
- 8 • Individual cellular level polymers level heterogeneity, distributions and stoichiometry ratios
9 changed in both PAOs and GAOs populations in response to changes in influent carbon and P
10 loading conditions.
- 11 • Intracellular polymeric stoichiometry evaluation within PAO populations enabled by Raman
12 analysis elucidated the phenotypic elasticity in PAOs depending on influent loading conditions
- 13 • Quantification of differentiated PHB and glycogen inclusion levels in PAOs and GAOs
14 showed that the influent rbCOD/P ratio increases, the excessive carbon beyond stoichiometric
15 requirement for PAOs was diverted into GAOs.
- 16 • Population-specific evaluation of intracellular polymers evidenced that P limiting conditions
17 at higher rbCOD/P ratios led to enhancement and increased reliance on glycolysis in addition
18 to partial/reverse TCA cycle for anaerobic reducing power generation.

19 These findings provided new insights into the metabolic diversity of the functionally relevant
20 populations in EBPR and population level formation for mechanistic EBPR model improvement
21 and development. It also demonstrated the potential of application of Raman method as a
22 powerful tool for the fundamental understanding of EBPR mechanism.

1 **Acknowledgement**

2 This study was funded by scholarship to ITRI-NU (Industrial Translational Research Initiative at
3 NU) from R&D of Veolia Water Solutions and Technologies, Sweden. Special thanks to Dr.
4 Thomas Welander for his support. We greatly thank Professor Max Diem, Dr. Tatyana
5 Chernenko and Ms. Evgenia Zuser in the department of Chemistry and Chemical Biology at
6 Northeastern University for their advice and assistance in Raman microscopic analysis. We
7 acknowledge Ms. Firouzeh Shiranian for her assistance with the monitoring of the lab-scale
8 SBR-EBPR.

9 **Supporting Information**

10 Additional supporting information has been included for clarification which are, STable 1:
11 Details on oligonucleotide probes used for FISH in this study and their respective target groups;
12 STable 2 : Performance of SBR-EBPR at different COD/P ratios studied; SFigure 1: Exemplary
13 P release and uptake profiles of batch testing for sludge from 3 different EBPR SBRs systems
14 fed with different influent COD/P ratios ; SFigure 2: Intracellular polymer abundance
15 distribution among individual GAO cells for PHB and glycogen polymers during batch testing
16 for different COD/P ratios; SFigure 3: Effect of sample size on Single Cell Raman Spectra
17 (SCRS); SFigure 4: Radial based function kernel and Eigen-decomposition used to investigate
18 the sufficient sampling size; SFigure 5: Flow of 1 C mol Acetate and the resulting stoichiometry
19 of intracellular polymers polyphosphate, PHB and glycogen in alternative anaerobic metabolic
20 pathways in EBPR for PHB formation (earlier models); SFigure 6: Redox balance strategies for
21 *Accumulibacter* under anaerobic conditions (recent understanding).

22

23

1 **References:**

- 2 Acevedo, B., Oehmen, A., Carvalho, G., Seco, A., Borrás, L., Barat, R., 2012. Metabolic shift of
3 polyphosphate-accumulating organisms with different levels of polyphosphate storage.
4 *Water Research* 46, 1889-1900.
5
- 6 Acevedo, B., Murgui, M., Borrás, L., Barat, R., 2017. New insights in the metabolic behavior of
7 PAO under negligible poly-P reserves. *Chemical Engineering Journal* 311, 82-90.
8
- 9 APHA, 1998. *Standard Methods for the Examination of water and wastewater*. 20th ed.;
10 American Public Health Association, Washington D.C.
11
- 12 Barnard, J., Shaw, A., Lindeke, D., 2005. In *Using Alternative Parameters to Predict Success for*
13 *Phosphorus Removal in WWTPs*, 73rd Annual Water Environment Federation Technical
14 *Exposition and Conference*, Washington DC, USA.
15
- 16 Broughton, A., Pratt, S., Shilton, A., 2008. Enhanced biological phosphorus removal for high
17 strength wastewater with a low rbCOD:P ratio. *Bioresource Technology* 99, 1236-1241.
18
- 19 Cech, J. S., Hartman, P., 1993. Competition between Polyphosphate and Polysaccharide
20 Accumulating Bacteria in Enhanced Biological Phosphate Removal Systems. *Water*
21 *Research* 27 (7), 1219-1225.
22
- 23 Daims, H., Lucker, S., Wagner, M., 2006. daime, a novel image analysis program for microbial
24 ecology and biofilm research. *Environmental Microbiology* 8(2), 200-213.
25
- 26 daSilva, L. G., Gamez, K. O., Gomes, J. C., Akkermans, K., Welles, L., Abbas, B., van
27 Loosdrecht, M. C. M., Wahl, S. A., 2018. Revealing metabolic flexibility of *Candidus*
28 *Accumulabacter phosphatis* through rediz cofactor analysis and metabolic network
29 modeling, bioRxiv Preprint.
30
- 31 Erdal, Z. K., 2002. *The Biochemistry of EBPR: Role of Glycogen in Biological Phosphorus*
32 *Removal and the Impact of the Operating Conditions on the Involvement of Glycogen*. PhD
33 *Dissertation*, Virginia Tech, Blacksburg, VA, USA.
34
- 35 Filipe, C.D.M., Daigger, G.T., Grady, C.P.L., 2001. pH as a key factor in the competition
36 between glycogen-accumulating organisms and phosphorus-accumulating organisms. *Water*
37 *Environ. Res.* 73 (2), 223-232.
38
- 39 Gu, A. Z., Saunders, A.M., Neethling, J.B., Stensel, H.D., Blackall, L., 2005. Investigation of
40 PAOs and GAOs and their effects on EBPR performance at full-scale wastewater treatment
41 plants in US. *Water Environment Research Foundation*: Alexandria, Virginia, USA.
42
- 43 Gu, A. Z., Saunders, A., Neethling, J. B., Stensel, H. D., Blackall, L. L., 2008. Functionally
44 Relevant Microorganisms to Enhanced Biological Phosphorus Removal Performance at

- 1 Full-Scale Wastewater Treatment Plants in the United States. *Water Environment Research*
2 80 (8), 688-698.
3
- 4 Gu, A. Z., 2018. PAO metabolic Pathways, Water Environment Federation Report.
5
- 6 He, S., Gu, A. Z., McMahon, K. D., 2008. Progress toward understanding the distribution of
7 *Accumulibacter* among full-scale enhanced biological phosphorus removal systems.
8 *Microbial Ecology* 55, (2), 229-236.
9
- 10 He, S. M., Kunin, V., Haynes, M., Martin, H. G., Ivanova, N., Rohwer, F., Hugenholtz, P.,
11 McMahon, K. D., 2010. Metatranscriptomic array analysis of '*Candidatus Accumulibacter*
12 *phosphatis*'-enriched enhanced biological phosphorus removal sludge. *Environmental*
13 *Microbiology* 12 (5), 1205-1217.
14
- 15 Jenkins, D., Richards, M.G., Daigger, G.T., 2003. *Manual on the Causes and Control of*
16 *Activated Sludge Bulking and Foaming*. 2nd edition, Lewis, London, UK.
17
- 18 Kong, Y.H., Beer, M., Rees, G.N., Seviour, R.J., 2002. Functional analysis of microbial
19 communities in aerobic-anaerobic sequencing batch reactors fed with different
20 phosphorus/carbon (P/C) ratios. *Microbiology* 148, 2299–2307.
21
- 22 Lanham, A. B., Oehmen, A., Saunders, A. M., Carvalho, G., Nielsen, P. H., Reis, M. A., 2013.
23 *Metabolic versatility in full-scale wastewater treatment plants performing enhanced*
24 *biological phosphorus removal*. *Water research* 47(19), 7032-7041.
25
- 26 Li, Y., Cope, H. A., Rahman, S. M., Li, G., Nielsen, P. H., Elfick A., Gu, A. Z., 2018. Toward
27 Better Understanding of EBPR Systems via Linking Raman-Based Phenotypic Profiling
28 with Phylogenetic Diversity *Environmental Science & Technology* 52 (15), 8596-8606.
29
- 30 Liu, W. T., Nakamura, K., Matsuo, T., Mino, T., 1997. Internal energy-based competition
31 between polyphosphate- and glycogen-accumulating bacteria in biological phosphorus
32 removal reactors - Effect of P/C feeding ratio. *Water Research* 31(6), 1430-1438.
33
- 34 Lopez-Vazquez, C.M., Oehmen, A., Hooijmans, C.M., Brdjanovic, D., Gijzen, H.J., Yuan, Z.,
35 van Loosdrecht, M.C.M., 2009. Modeling the PAO GAO competition: effects of carbon
36 source, pH and temperature. *Water Res.* 43 (2), 450-462.
37
- 38 Majed, N., Matthaus, C., Diem, M. and Gu, A.Z., 2009. Evaluation of Intracellular
39 Polyphosphate Dynamics in Enhanced Biological Phosphorus Removal Process Using
40 Raman Microscopy. *Environmental Science & Technology* 43, (11), 5436-5442.
41
- 42 Majed, N., Gu, A. Z., 2010. Application of Raman Microscopy for Simultaneous and
43 Quantitative Evaluation of Multiple Intracellular Polymers Dynamics Functionally Relevant
44 to Enhanced Biological Phosphorus Removal Processes. *Environmental Science &*
45 *Technology* 44 (22), 8601-8608.

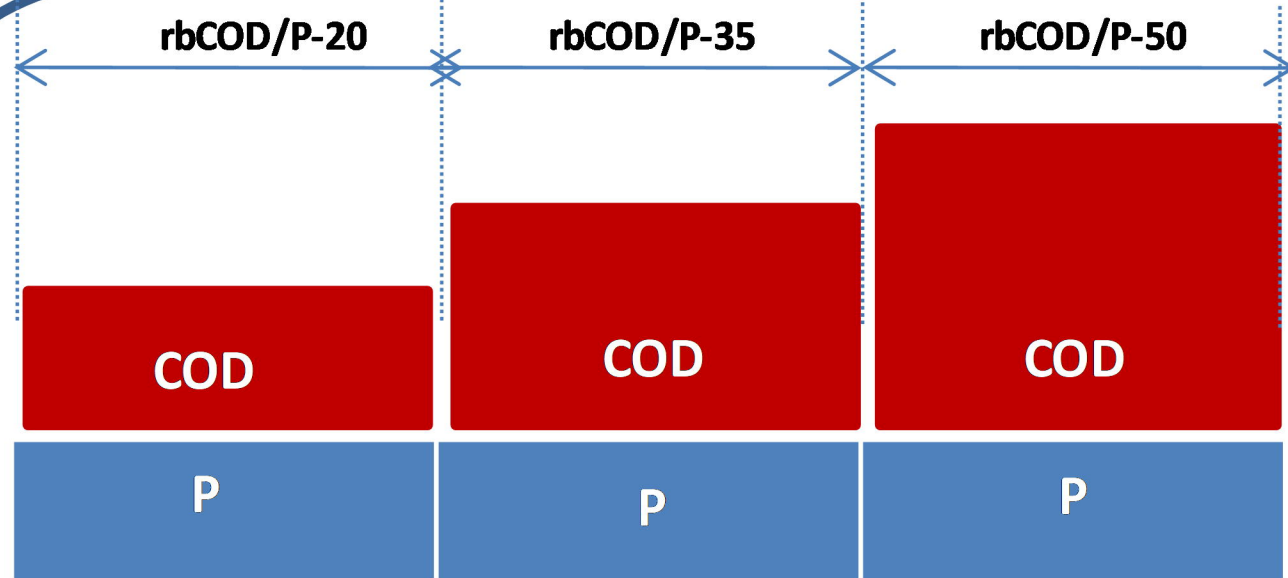
- 1
2 Majed, N., Chernenko, T., Diem, M., Gu, A. Z., 2012. Identification of functionally relevant
3 populations in enhanced biological phosphorus removal processes based on intracellular
4 polymers profiles and insights into the metabolic diversity and heterogeneity.
5 *Environmental Science & Technology* 46, 5010-5017.
6
- 7 Martin, H. G., Ivanova, N., Kunin, V., Warnecke, F., Barry, K. W., McHardy, A. C., Yeates, C.,
8 He, S. M., Salamov, A. A., Szeto, E., Dalin, E., Putnam, N. H., Shapiro, H. J., Pangilinan, J.
9 L., Rigoutsos, I., Kyrpides, N. C., Blackall, L. L., McMahon, K. D., Hugenholtz, P., 2006.
10 Metagenomic analysis of two enhanced biological phosphorus removal (EBPR) sludge
11 communities. *Nature Biotechnology* 24 (10), 1263-1269.
12
- 13 Muszyński, A., Miłobędzka, A., 2015. The effects of carbon/phosphorus ratio on polyphosphate-
14 and glycogen-accumulating organisms in aerobic granular sludge. *International Journal of*
15 *Environmental Science and Technology* 12(9), 3053-3060.
16
- 17 Neethling, J. B., Bakke, B., Benisch, M., Gu, A. Z., Stephens, S., Stensel, H. D., 2005. Factors
18 Influencing the Reliability of Enhanced Biological Phosphorus Removal. report 01-CTS-3;
19 Water Environment Research Foundation: Alexandria, Virginia, UK.
20
- 21 Oehmen, A., Lemos, P. C., Carvalho, G., Yuan, Z. G., Keller, J., Blackall, L. L., Reis, M. A. M.,
22 2007. Advances in enhanced biological phosphorus removal: From micro to macro scale.
23 *Water Research* 41, (11), 2271-2300.
24
- 25 Oehmen, A., Carvalho, G., Lopez-Vazquez, C. M., van Loosdrecht, M. C. M., Reis, M. A. M.,
26 2010. Incorporating microbial ecology into the metabolic modelling of polyphosphate
27 accumulating organisms and glycogen accumulating organisms. *Water Research* 44 (17),
28 4992-5004.
29
- 30 Randall, C.W., Barnard, J.L., Stensel, D.H., 1992. Design and Retrofit of Wastewater Treatment
31 Plants for Biological Nutrient Removal. Technomic Publishing Co, Lancaster, PA.
32
- 33 Saunders, A. M., Oehmen, A., Blackall, L. L., Yuan, Z., Keller, J., 2003. The effect of GAOs
34 (glycogen accumulating organisms) on anaerobic carbon requirements in full-scale
35 Australian EBPR (enhanced biological phosphorus removal) plants. *Water Science and*
36 *Technology* 47(11), 37-43.
37
- 38 Schuler, A. J., Jenkins, D., 2003. Enhanced biological phosphorus removal from wastewater by
39 biomass with different phosphorus contents, part I: Experimental results and comparison
40 with metabolic models. *Water Environ Res* 75(6), 485-498.
41
- 42 Schuler, A. J., 2005. Diversity matters: Dynamic simulation of distributed bacterial states in
43 suspended growth biological wastewater treatment systems. *Biotechnol. Bioeng.* 91 (1),
44 62– 74.
45

- 1 Smolders, G. J. F., Vandermeij, J., Vanloosdrecht, M. C. M., Heijnen, J. J., 1994. Model of the
2 Anaerobic Metabolism of the Biological Phosphorus Removal Process - Stoichiometry and
3 pH Influence. *Biotechnology and Bioengineering* 43(6), 461-470.
4
- 5 Stephens, H. M., Neethling, J. B., Benischer, M., Gu, A. Z., Stensel, H. D., 2004.
6 Comprehensive analysis of full-scale enhanced biological phosphorus removal facilities.,
7 Water Environment Federation 77th Annual Conference and Exposition, New Orleans, LA,
8 USA.
9
- 10 Streichan, M., Golecki, J.R., Schon, G., 1990. Polyphosphate-accumulating bacteria from
11 sewage plant with different processes of biological phosphorus removal. *FEMS Microbiol.*
12 *Ecol.* 73, 113– 124.
13
- 14 Tchobanoglous, G., Burton, F.L., Stensel, H.D., 2003. In: Eddy, Ma (Ed.), *Wastewater*
15 *Engineering: Treatment and Reuse*. McGraw-Hill, New York, NY.
16
- 17 Tetreault, M. J., Benedict A. H., Kaempfer, C., Borth, E. F., 1986. Biological Phosphorus
18 Removal: A Technology Evaluation. *J. Water Pollut. Control Fed.*, 58, 823–837.
19
- 20 Tu, Y., Schuler, A.J., 2013. Low acetate concentrations favor polyphosphate-accumulating
21 organisms over glycogen accumulating organisms in enhanced biological phosphorus
22 removal from wastewater. *Environ. Sci. Technol.* 47 (8), 3816-3824.
23
- 24 Whang, L. M., Park, J. K., 2006. Competition between polyphosphate- and glycogen-
25 accumulating organisms in enhanced-biological-phosphorus-removal systems: Effect of
26 temperature and sludge age. *Water Environment Research* 78, (1), 4-11.
27
- 28 Wilmes, P., Andersson, A. F., Lefsrud, M. G., Wexler, M., Shah, M., Zhang, B., Hettich, R. L.,
29 Bond, P. L., VerBerkmoes, N. C., Banfield, J. F., 2008. Community proteogenomics
30 highlights microbial strain-variant protein expression within activated sludge performing
31 enhanced biological phosphorus removal. *Isme Journal* 2(8), 853-864.
32
- 33 Zeng, R. J., Saunders, A. M., Yuan, Z. G., Blackall, L. L., Keller, J., 2003. Identification and
34 comparison of aerobic and denitrifying polyphosphate-accumulating organisms." *Biotechnol*
35 *Bioeng* 83(2), 140-148.
36
- 37 Zhou, Y., Pijuan, M., Zeng, R. J., Yuan, Z. G., 2009. Involvement of the TCA cycle in the
38 anaerobic metabolism of polyphosphate accumulating organisms (PAOs). *Water Research*
39 43(5), 1330-1340.
40
- 41 Zhou, Y., Pijuan, M., Oehmen, A., Yuan, Z. G., 2010. The source of reducing power in the
42 anaerobic metabolism of polyphosphate accumulating organisms (PAOs) - a mini-review.
43 *Water Science and Technology* 61(7), 1653-1662.
44

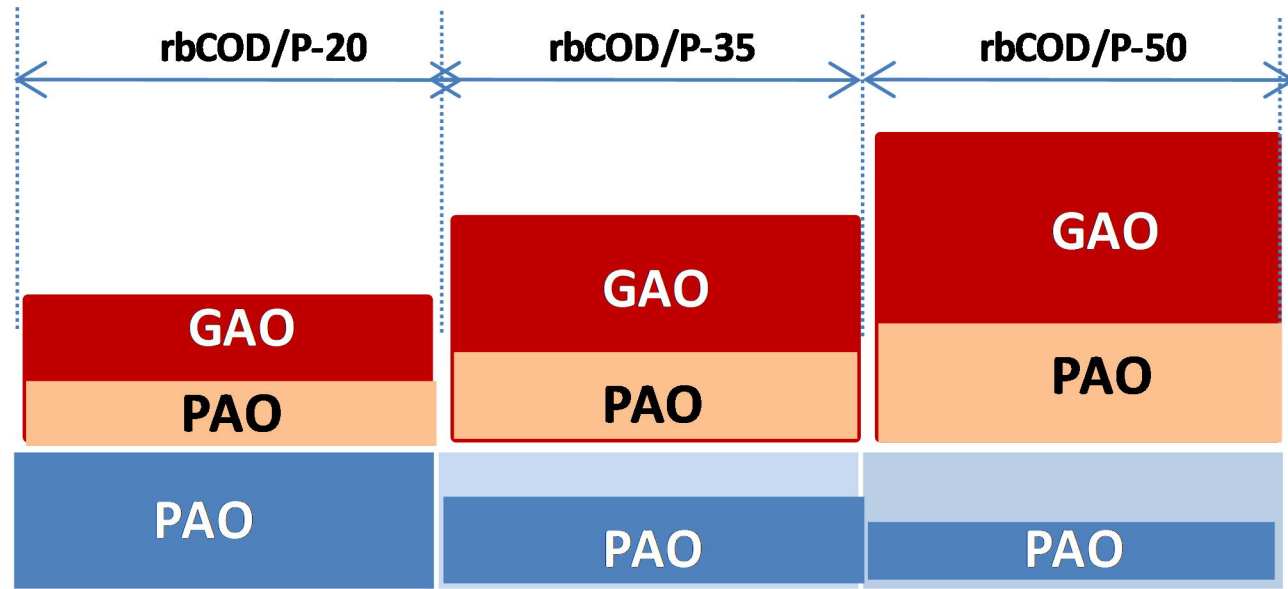
1 Zilles, J. L., Peccia, J., Kim, M. W., Hung, C. H., Noguera, D. R., 2002. Involvement of
2 Rhodocyclus-related organisms in phosphorus removal in full-scale wastewater treatment
3 plants. *Applied and Environmental Microbiology* 68 (6), 2763-2769.

4
5

6

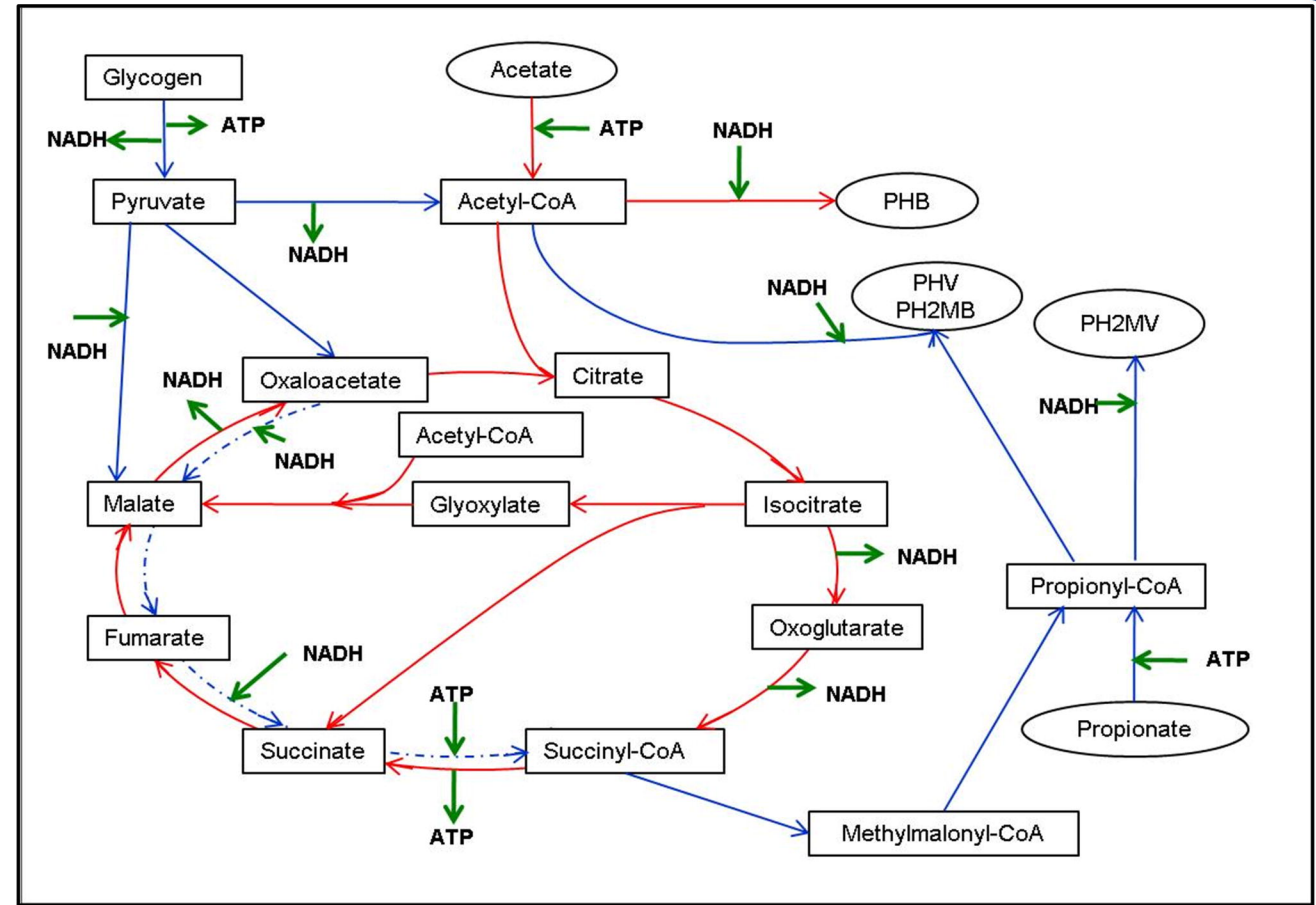


Influent rbCOD and P

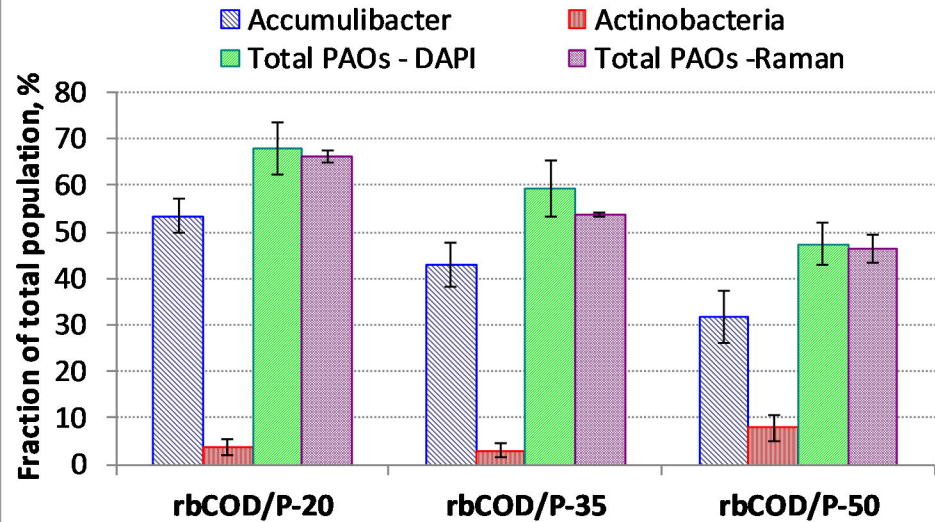


Intracellular polyP and carbon distribution

Carbon
PolyP



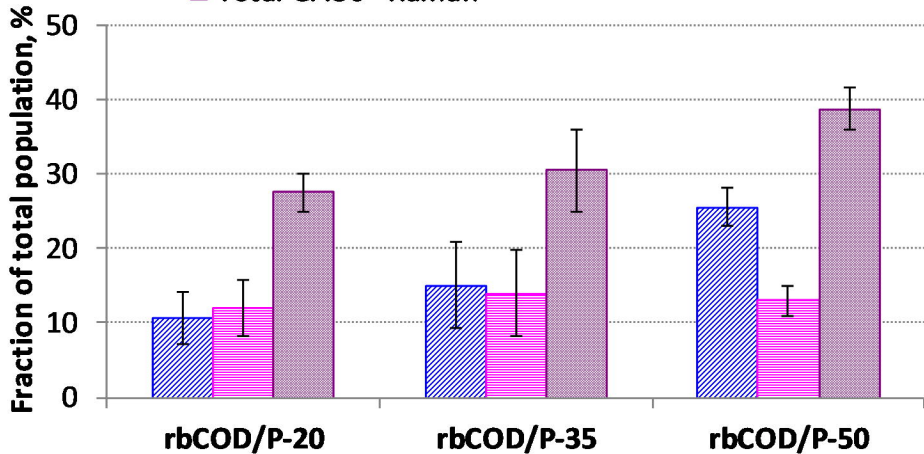
Schematic of anaerobic biochemical pathways employed by PAOs for energy (ATP) and reducing power (NADH) production and for intracellular PHAs formation. Possible pathways proposed include different extent and combinations of the glycolysis pathway (blue line), succinate-propionate pathway (blue dotted line), partial or full TCA cycle pathway (red line).

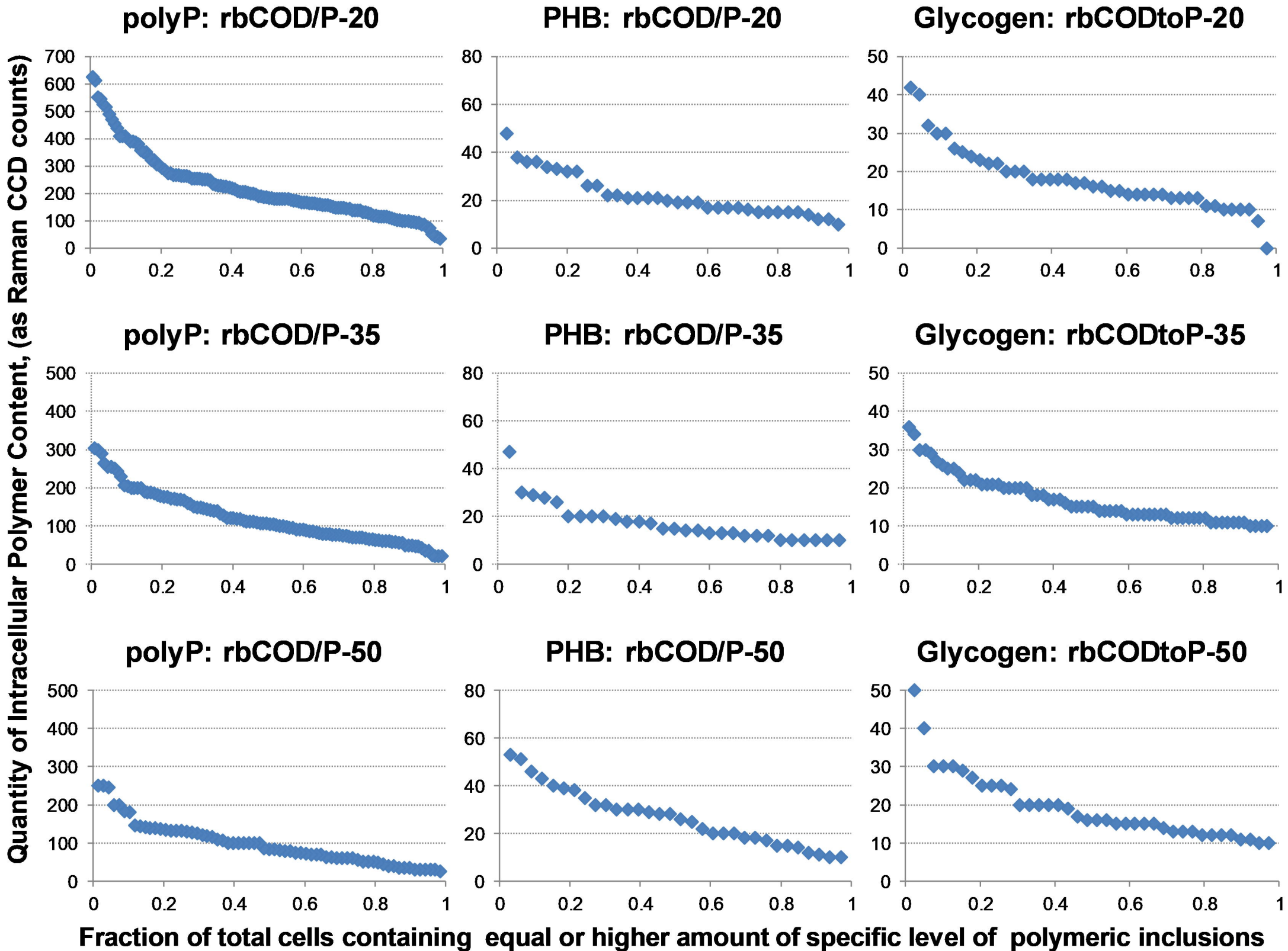


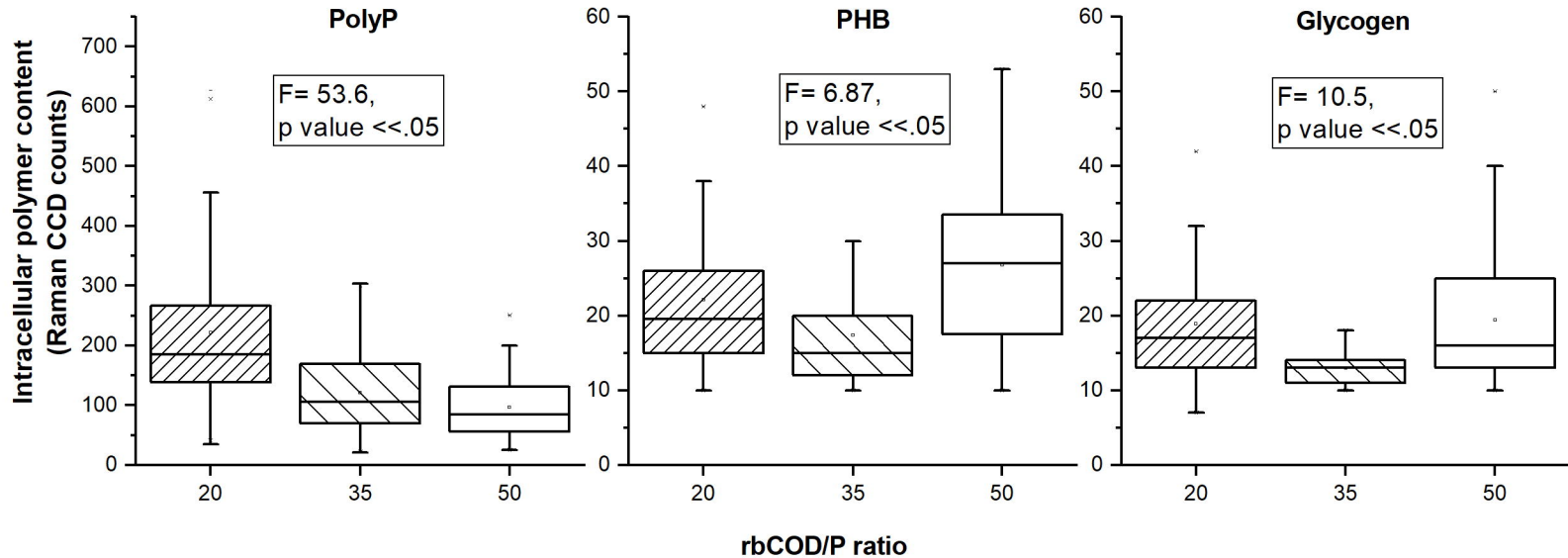
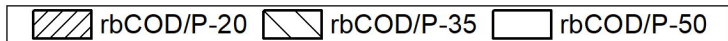
Competibacter

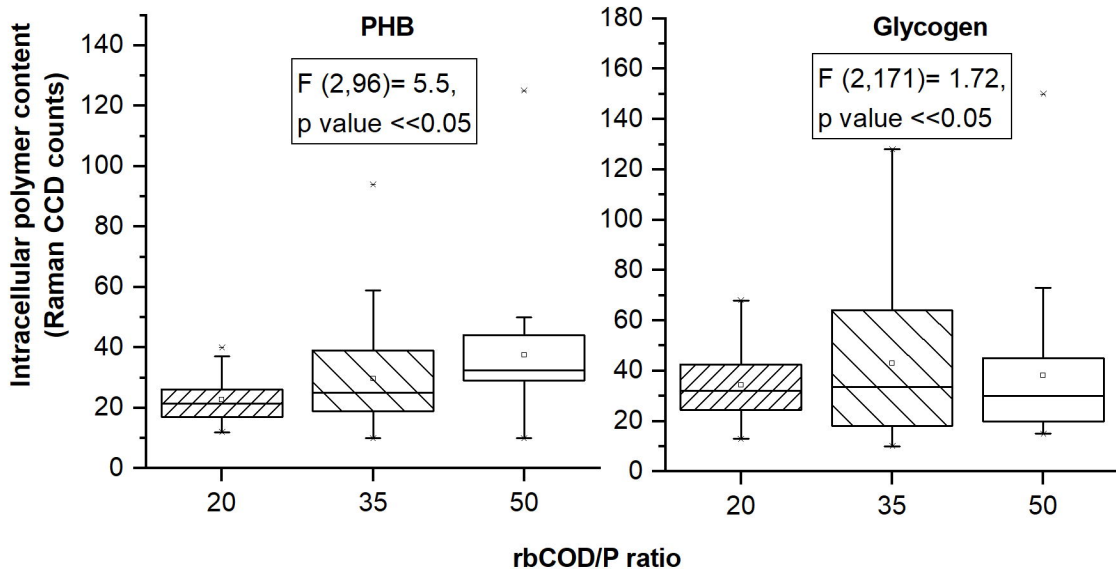
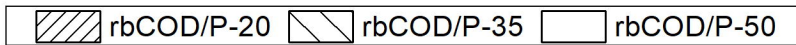
Defluvicoccus cluster 2

Total GAOs - Raman



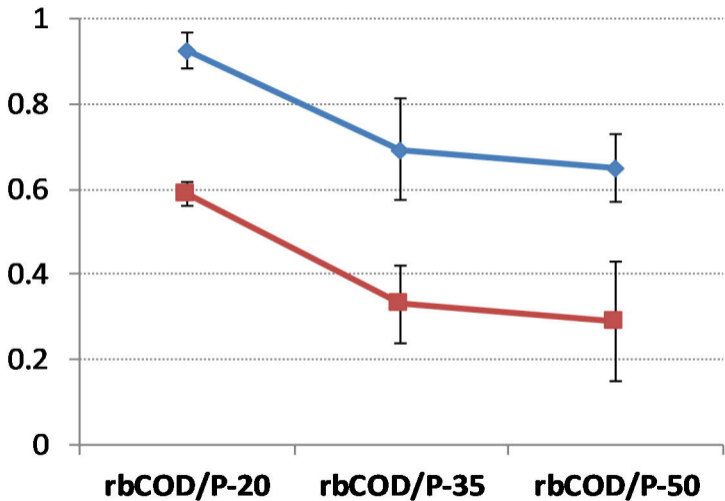






◆ PHB(PAO)/ PHB(GAO) ■ Gly(PAO)/ Gly(GAO)

**PHB and Glycogen inclusion ratio
between PAO/GAO, CCD/CCD**



rbCOD/P-20

rbCOD/P-35

rbCOD/P-50

COD

COD

COD

P

P

P

Influent rbCOD and P

rbCOD/P-20

rbCOD/P-35

rbCOD/P-50

GAO

PAO

PAO

GAO

PAO

PAO

GAO

PAO

PAO

Carbon

polyp

Intracellular polyP and carbon distribution

Maximum PHB/Glycogen concentration
in anaerobic phase, Raman CCD/100 cell

900
800
700
600
500
400
300
200
100
0

Total PHB(PAO)
Total Gly(PAO)

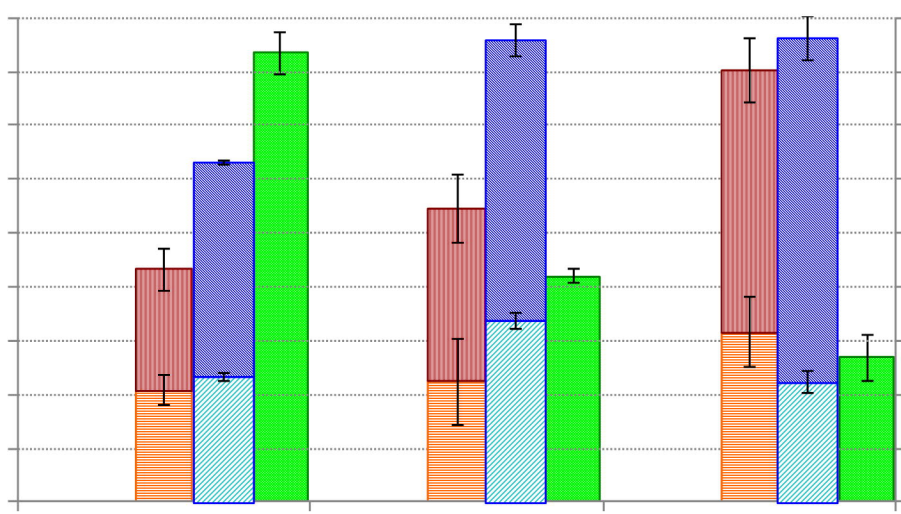
Total PHB(GAO)
Total Gly(GAO)

Total polyP(PAO)

rbCOD/P-20

rbCOD/P-35


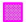
rbCOD/P-50



6300
5600
4900
4200
3500
2800
2100
1400
700
0

Maximum polyP concentration in
aerobic phase, Raman CCD/100 cell

**Fraction of total PAOs with
specific inclusions, %**

-  Glycogen containing PAOs at aerobic end
-  PHV containing PAOs at anerobic end

